Near Field Effects of a Hidden Seismic Fault underlying Concrete Dam

T. Ohmachi[1], N. Kojima[2], A. Murakami[3], and N. Komaba[4]

1) Professor, Department of Built Environment, Tokyo Institute of Technology, Japan
2) Civil Engineer, Metropolitan Expressway Public Corporation, Japan (Formerly, Graduate Student, Ditto)
3) Engineer, Sumisho Electronics Co. Ltd, Japan (Formerly, Graduate Student, Ditto)
4) Graduate Student, Department of Environmental Science and Technology, Tokyo Institute of Technology, Japan
ohmachi@enveng.titech.ac.jp, kojima.n@mex.go.jp, murakamiatushi@kuramae.ne.jp, komaban@depe.titech.ac.jp

Abstract: The 2000 Western Tottori earthquake (M_J 7.3), Japan, was caused by a hidden seismic fault underlying Kasho Dam, a 46 m-high concrete gravity dam. Strong-motion accelerometers registered peak accelerations of 2051 and 531 gal at the top of the dam and in the lower inspection gallery, respectively. Integration of the acceleration records in the gallery gives a permanent displacement of 28 cm to the north, 7 cm to the west, and uplift of 5 cm. The dam survived the earthquake without serious damage, but the reservoir water level dropped suddenly by 6 cm, followed by damped free vibration that continued for several hours. Based on numerical simulation and field observation, the water level change is attributed to ground displacement in the near field followed by seiching of the reservoir. The vibration period in the upstream-downstream direction of the dam changed noticeably during the main shock, probably due to hydrodynamic pressure variations.

1. INTRODUCTION

The 2000 Western Tottori earthquake (M_J 7.3), Japan, occurred at 13:30 (local time) on October 6, 2000. Kasho Dam which lies in the near field of this earthquake, is a concrete gravity dam with height of 46.4 m and crest length of 174 m, constructed in 1989. The full water level of the reservoir is EL 118 m; at the time of the main shock the water level was EL 112 m.

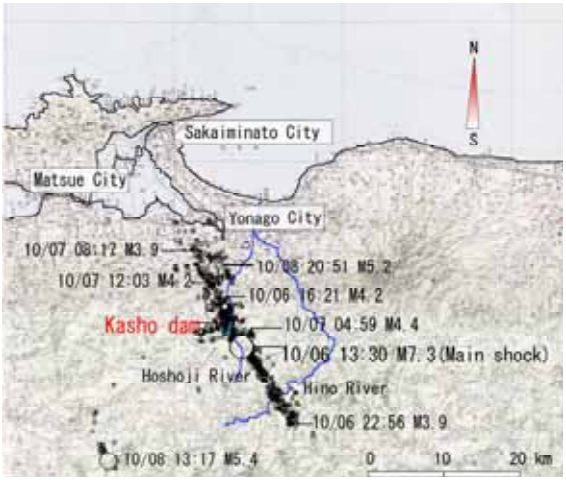

Fig. 1 Map showing locations of the main shock, aftershocks, and Kasho Dam

Strong motion accelerometers at the dam registered peak accelerations of 2051 and 531 gal at the top of the dam and in the lower inspection gallery, respectively (Japan Commission on Large Dams, 2002). Despite such high acceleration, the dam body escaped serious damage. Although no increase in water leakage was observed, the reservoir water level of the dam recorded a sudden drop of 6 cm immediately after the main shock, followed by damped free vibration that continued for several hours. The drop in reservoir water level was not only a mystery but also raised concern among dam engineers.

The location of the dam is shown in Fig. 1, along with the locations of hypocenters of the main

shock and aftershocks. The seismic fault appears to run through the Kasho Dam site. No clear trace of fault rupturing was observed on the ground surface in the epicentral area (Inoue et al., 2002). The earthquake therefore appears to have been caused by seismic rupturing of a hidden fault underlying the dam site. This paper is reproduction of the authors' publication (Ohmachi et. al., 2003).

2. NEAR-FIELD GROUND DISPLACEMENT

2.1 Ground displacement inferred from strong-motion records

Three-component strong-motion accelerometers (seismometers) are installed firmly with bolts on the concrete floor of the upper elevator room at EL 124.4 m, and on the concrete floor of the lower inspection gallery at EL 87.0 m, as shown in Fig. 2. The horizontal components of both accelerometers are set N-S and E-W (the dam axis is oriented N110ºE). A floating reservoir water-level meter is also installed in a concrete well 0.8 m in diameter.

Acceleration records of the main shock captured at the two seismometer installations are shown in Fig. 3. The earthquake acceleration was sampled at 100 Hz with 24-bit resolution, with a reliable frequency range of DC to 41 Hz. Seismic ground displacement was estimated by integrating the acceleration histories at the lower inspection gallery twice with respect to time.

The result in Fig. 4 shows that the dam underwent different modes of displacement in the three directions. In the N-S direction, the dam displaced linearly to the north with a final permanent displacement of 27.6 cm. In the E-W direction, the displacement varied sinusoidally, with a final permanent displacement of 6.5 cm to the west. In the vertical direction, the displacement exhibited a sharp upward peak, with a final permanent uplift of 4.7 cm.

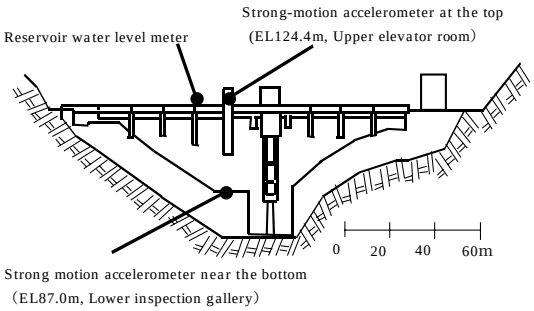

Fig. 2 Locations of strong-motion accelerometers and water level meter at Kasho Dam

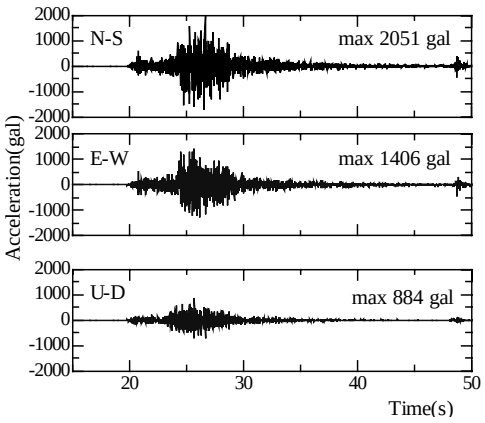

(a) Top of the dam (EL 124.4m)

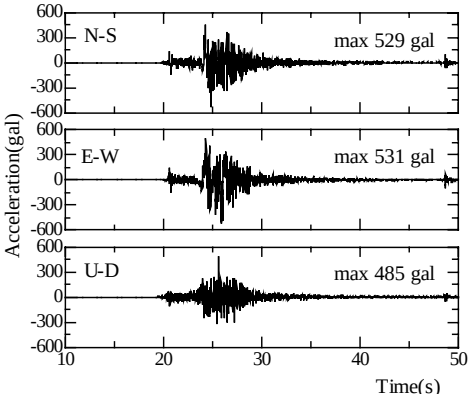

(b) Lower inspection gallery (EL 87.0m)

Fig. 3 Strong-motion acceleration of the main shock recorded at Kasho Dam

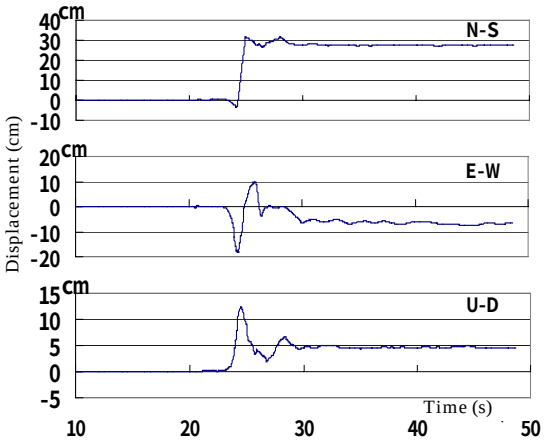

Fig. 4 Displacement histories obtained by integration of acceleration records

2.2 Ground displacement from numerical simulation

Using the fault parameters shown in Table 1 (Geographical Survey Institute, 2000), the ground displacement associated with the seismic faulting event was simulated using the 3D boundary element method (BEM). The seismic fault of the main shock was a left lateral strike slip fault with strike of N152ºE.

The simulation was conducted for a rectangular area of 23 km long (N-S) by 17 km wide (E-W), encompassing Kasho Dam and its reservoir. The ground was simplified as a half-space of homogenous elasticity with shear wave velocity of 4 km/s. In the first step of the simulation, seismic ground displacement was calculated at every node of a 500 m × 500 m mesh. The result is shown in Fig. 5, where thick broken lines indicate the projection of the fault plane, thick solid lines denote the reservoir, and thin solid lines are the lines of equal displacement. The iso-displacement lines are almost parallel to the fault projection in the vicinity of the reservoir, indicating uplift to the northeast of the reservoir and settlement to the southwest.

The displacement in the area indicated by the solid lines in Fig. 5(a) was interpolated, with the result as shown in Fig. 5(b). The profile of the reservoir is drawn along the altitude of the design flood water level (EL123.2 m). Kasho Dam is located at the north end of the reservoir.

The histories of ground displacement around the dam obtained from the interpolation of the simulated displacement are plotted in Fig. 6. The histories appear very similar to the recorded displacement histories in Fig. 4, although the amplitudes are slightly smaller. The simulated permanent ground displacement at the dam is 10.9 cm to the north and 0.1 cm to the west, with uplift of 2.5 cm. The horizontal displacements shown in Figs. 4 and 6 are plotted in Fig. 7 in terms of motion trajectories. It is interesting to note that both trajectories in Fig. 7 have common features, such as the direction of initial motion, elliptic motion in the final stage, and a large transient shift to the NE or NNE.

Table 1 Fault parameters used for simulation

Strike (deg.)	**152**
Dip (deg.)	**86**
Rake (deg.)	**-7**
Dislocation (m)	**1.4**
Depth of fault (m)	**1**
Fault length (km)	**20**
Fault width (km)	**10**

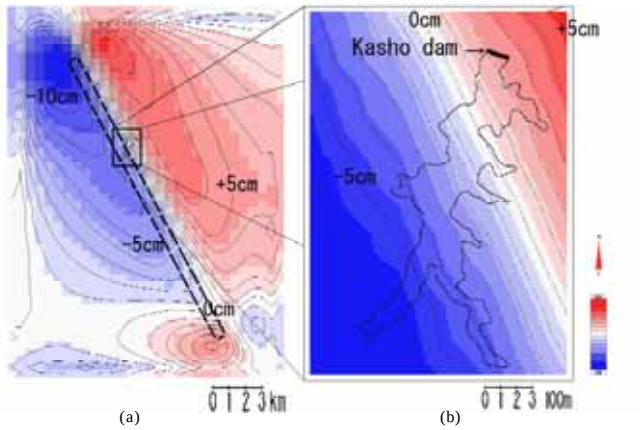

Fig. 5 Vertical ground displacement evaluated from simulation by (a) BEM and (b) its interpolation

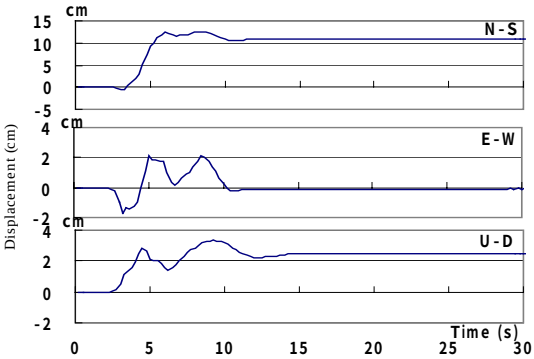

Fig.6 Ground displacement at Kasho Dam simulated by BEM

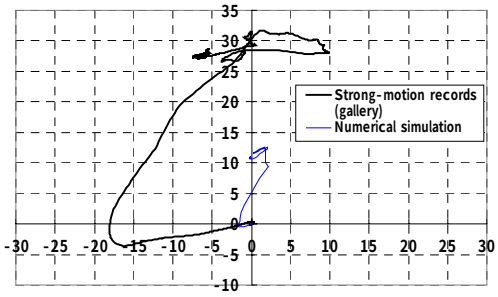

Fig. 7 Horizontal displacement motion trajectories estimated from strong-motion records and the simulation

2.3 Comparison of vertical displacements from simulation and ground survey

Following the main shock, a ground survey was conducted at 65 points along the reservoir as shown in Fig. 8, in which straight lines A to D are parallel to the fault projection shown in Fig. 5. Taking the distance from line A as a reference, the vertical displacements from the simulation and the survey are shown in Fig. 9. The displacements from the survey are almost three times that indicated by the simulation, and larger particularly between lines B and C. The differences could be attributed to several factors such as inaccurate parameters used in the simulation and the effects of local site conditions, as well as the effect of the many aftershocks, which were not considered in the simulation.

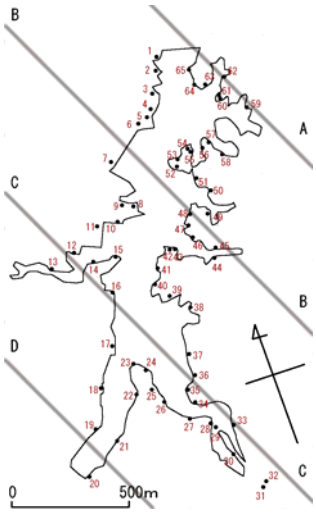

Fig. 8 Observation points along the reservoir for the ground survey

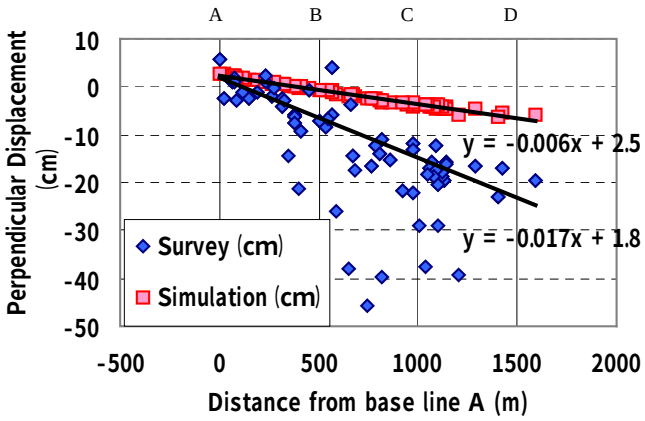

Fig. 9 Comparison of vertical displacements evaluated from the simulation and survey

2.4 Comparison with readings of a plumb line

To detect relative displacement between the top and bottom of the dam, a plumb line is installed in a vertical shaft 30 cm in diameter. The upper end of the steel plumb line is fixed to the floor of the upper elevator room, next to the strong motion accelerometer, and the weight on the lower end is housed in a measurement device located at EL 89.5 m in the lower inspection gallery. Automatic measurement is usually conducted only a few times a day. Readings from the measurement during October 3 and October 13 are plotted in Fig. 10. The main shock induced a relative displacement of –2.8 mm in the *x* (right-bank) direction, and 0.7 mm in the *y* (upstream) direction, with a resultant displacement of 2.9 mm.

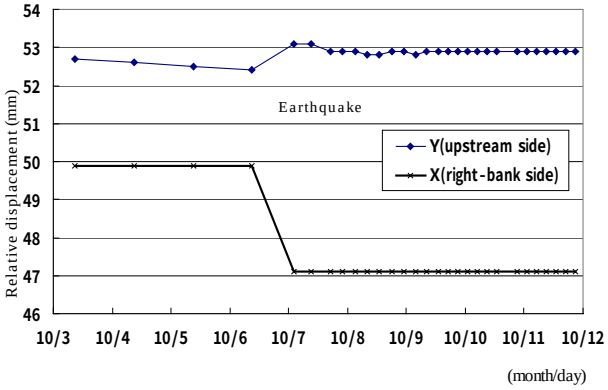

Fig. 10 Relative displacement evaluated from plumb line readings

If the relative displacement indicated by the plumb line readings is attributed to an inclination of the dam body caused by earthquake-induced ground displacement of the dam foundation, the inclination will be quantitatively given by the resultant displacement divided by the length of the plumb line; $2.9/34900 = 8.3 \times 10^{-5}$. In the vicinity of the dam, the inclination of the earthquake-induced ground displacement estimated from the simulation is 6×10^{-5}, as shown in Fig. 9. Although this differs slightly from the inclination determined from readings of the plumb line in terms of magnitude and direction of inclination, it is reasonable to surmise that the dam site was

displaced by the seismic faulting of the main shock, as inferred from integration of the strong-motion acceleration.

3. CHANGE IN RESERVOIR WATER LEVEL

3.1 Records of reservoir water level

The reservoir water level is continuously recorded, and the history around the time of the earthquake is shown in Fig. 11. The upper and lower histories in Fig. 11 are the records with low and high resolutions, respectively. The records indicate that the water level dropped suddenly by about 6 cm at the time of the main shock, followed by damped free vibration that continued for several hours.

The water level record was roughly reproduced from the readings of successive peaks and troughs of the original record. The Fourier spectrum of the reproduced history is shown in Fig. 12, which shows the free-vibration period of 6.5 min and a damping ratio of 2%.

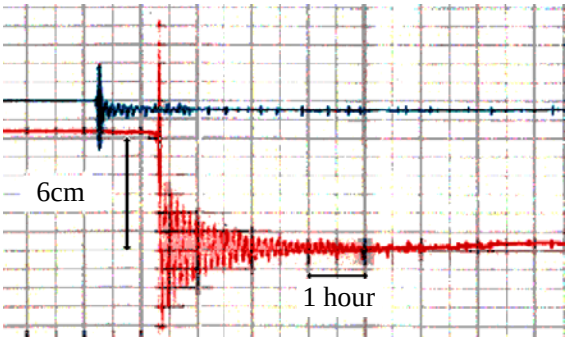

Fig. 11 Records of reservoir water level at Kasho Dam

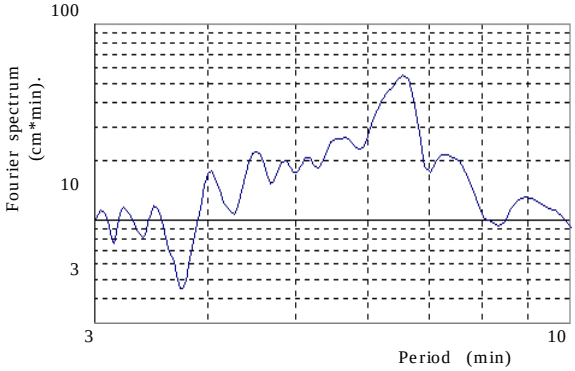

Fig. 12 Reproduced free-vibration history of the corresponding spectrum

3.2 Cause of the sudden drop in reservoir water level

The seismic faulting gave rise to uplift of the dam body and a change in the ground slope of the base of the reservoir as a result of near-field ground displacement. These factors are regarded to be the main cause of the sudden drop in reservoir water level. A schematic explanation is shown in Fig. 13, where the dam and ground slope before and after the main shock are indicated by thin and thick lines, respectively. In the figure, ΔH_1 is the water level change due to the increased reservoir capacity estimated from the average settlement of the reservoir area, and ΔH_2 is the water level change due to uplift of the dam. Using the simulated displacement shown in Fig. 5, ΔH_1 and ΔH_2 are –1.5 and 2.5 cm, respectively, with a corresponding water level change of –4.0 cm ($\Delta H = \Delta H_1 + \Delta H_2$), in reasonable agreement with the observation of –6.0 cm.

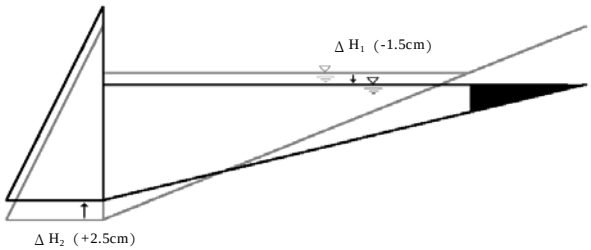

Fig. 13 Schematic explanation of water level change caused by ground displacement

3.3 Seiching of the reservoir

Free vibration of a water body such as a reservoir is referred to as seiching (Lamb, 1932). The fundamental period T for a rectangular reservoir is approximated by

$$T = \frac{2a}{\sqrt{gh}} \tag{1}$$

where a and h are the length and depth of the reservoir, and g is acceleration due to gravity. Introducing a 2 km and h 10 m into Eq. (1) for Kasho Dam gives a period of T 7.0 min, which is fairly close to the observed period of free vibration (6.5 min). Accordingly, the free vibration is thought to be mainly due to the fundamental mode of the seiche. Based on this result, the seiching was simulated using a numerical technique recently developed for tsunami simulation (Ohmachi et al., 2001). The technique basically involves solving the Navier-Stokes equation for the system using a 3D finite difference method (FDM).

In the present simulation, for the sake of simplicity, the dam and ground were assumed to be rigid. The initial water surface was supposed to have the same slope as that given from the simulated ground displacement, and then it was released under the force of gravity to induce free vibration of the reservoir. The water level history at the dam is shown in Fig. 14, from which the period of the simulated seiche is found to be 7.5 min (450 s).

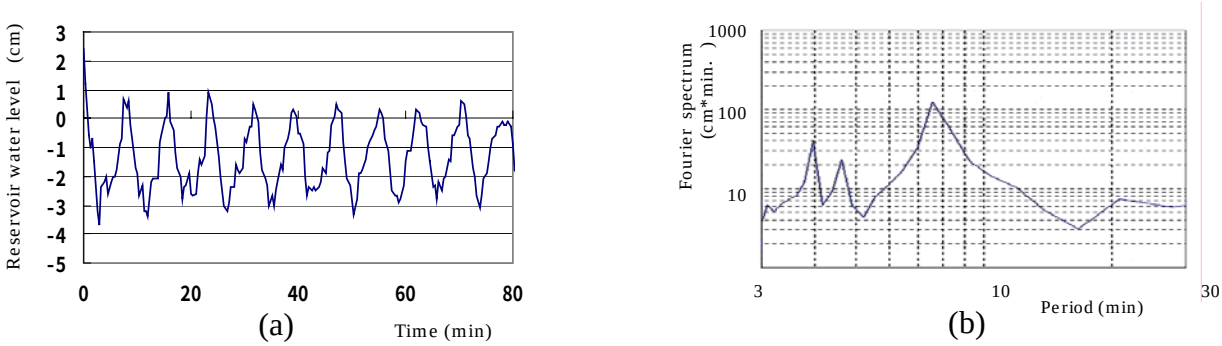

Fig. 14 History of simulated seiche at Kasho Dam

4. CHANGE IN VIBRATION PERIOD OF THE DAM

The response characteristics of the dam were analyzed by transforming the two horizontal components of the strong-motion records in the N-S and E-W directions shown in Fig. 3 into the upstream-downstream and dam-axis directions. The transformed acceleration histories are shown in Fig. 15. After transformation, the peak accelerations at the top of the dam were 2100 and 1684 gal in the upstream-downstream and dam-axis directions, respectively, and the peak accelerations in the lower inspection gallery were 503 and 570 gal.

The acceleration histories were divided into four 5.12-s samples as indicated in Fig. 15. At the top of the dam, peak accelerations in the upstream-downstream direction in these time segments were 491, 2100, 531 and 227 gal. The amplification factors between the top and the lower gallery, calculated by taking the Fourier spectral ratios between pairs of segments, are

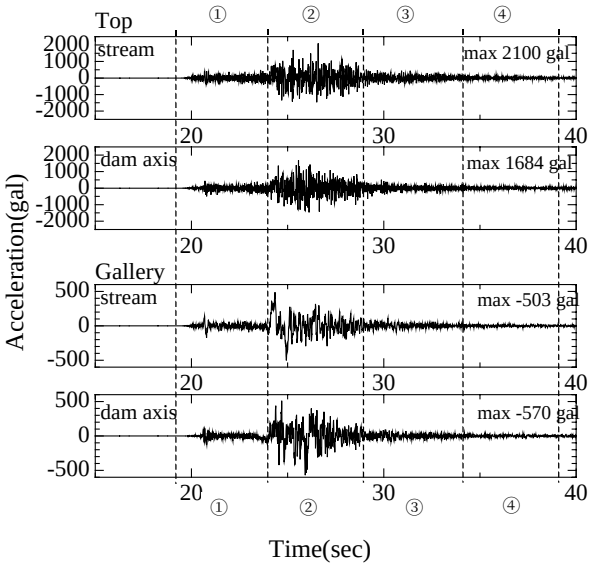

Fig. 15 Horizontal strong-motion records rotated with the azimuth of Kasho Dam

shown in Fig. 16. In the upstream-downstream direction shown, the main peak is at around 0.1 s, which appears to be associated with the fundamental mode of dam vibration. The peak periods of these amplification factors are 0.84, 0.96, 0.92 and 0.87 s for segments 1 through 4. Thus, during the main shock, the peak period was initially lengthened and then shortened, with a change exceeding 10%.

Lengthening of the vibration period during strong earthquake shaking is often caused by non-linearity of material properties. In the present case, however, because the lengthening is seen in the upstream-downstream direction only, and the period shortened shortly after, factors other than the non-linear properties seem to be responsible for the change in the period. One of the probable factors is hydrodynamic pressure acting on the upstream face of the dam, which would change in proportion to the intensity of earthquake acceleration (Westergaard, 1933).

At Kasho Dam, strong-motion acceleration was well recorded during not only the main shock but also aftershocks as listed in Table 2 (Japan Commission on Large Dams, 2002), which shows peak accelerations for the upstream-downstream direction. It should be noted in Table 2 that the reservoir water level at the time of the earthquakes was almost at the same, between EL 112.20 m and EL 110.93 m. From the acceleration records of the aftershocks, the peak periods in the upstream-downstream direction were similarly obtained and plotted against peak accelerations at the top of the dam, with the result as shown in Fig. 17. The peak period tends to increase with peak acceleration, as indicated by a broken line in the figure, although the plotted periods are somewhat scattered. Further study is therefore necessary in order to identify with certainty the factors responsible for the period change.

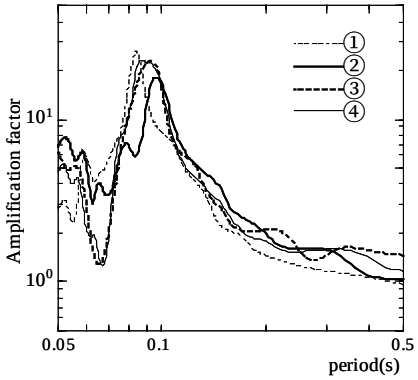

(a) Upstream-downstream direction

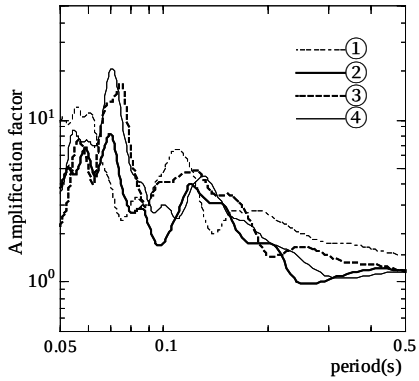

(b) Dam-axis direction

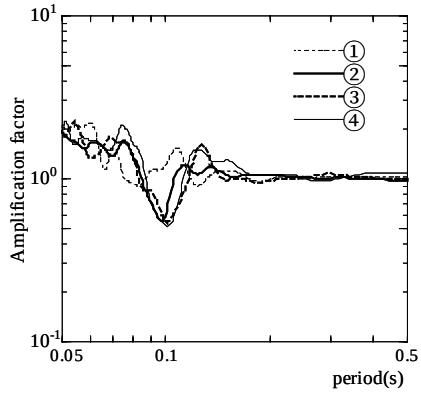

(c) Vertical direction

Fig. 16 Amplification factors between the dam top and the lower inspection gallery

Table 2 Main shock and aftershocks recorded at Kasho Dam in the 2000 Western Tottori earthquake

Date and time (M/Day)	M_J	Peak Acceleration (gal)		Water Depth (m)
		Top	Gallery	
10.06 13:30:00	7.3	2100	503	34.20
10.07 12:14:10	3.5	332	48	34.18
10.07 18:32:00	3.9	410	73	34.18
10.08 20:51:00	5.3	142	27	34.13
10.09 19:49:40	3.5	212	33	33.95
10.10 02:26:00	3.4	247	36	33.92
10.10 21:57:50	4.4	247	57	33.73
10.12 03:53:20	3.6	52	7	33.33
10.12 08:41:40	3.6	45	6	33.28
10.12 17:07:20	3.5	126	14	33.16
10.13 10:44:10	3.6	91	16	32.93

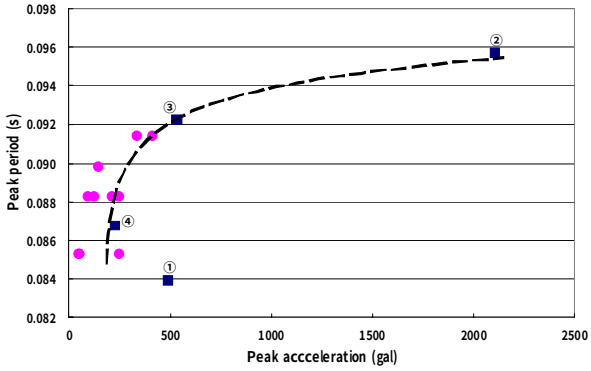

Fig. 17 Peak periods of the dam in the upstream-downstream direction

5. CONCLUSIONS

Kasho Dam, a concrete gravity dam, was located in the near field of the 2000 Western Tottori earthquake (M_J 7.3), which was caused by a hidden seismic fault. The strong-motion acceleration at the dam exceeded 2000 gal at the top of the dam and 500 gal in the lower inspection gallery during the main shock. Despite such large acceleration, the dam survived the earthquake without serious damage. However, the reservoir water level dropped considerably immediately after the main shock, and the vibration period of the dam varied by more than 10% during the main shock. The causes and effects of these observations were investigated in the present study, with the following conclusions.

The seismic rupturing of the hidden fault gave rise to not only dynamic but also permanent displacements at the dam site. Integration of the strong-motion acceleration observed in the lower inspection gallery gave a permanent displacement of 28 cm to the north, 7 cm to the west, and uplift of about 5 cm.

The sudden 6-cm drop in reservoir water level observed immediately after the main shock has been attributable to the permanent displacement of the ground in the near field of the earthquake. The free vibration of the reservoir water level following the sudden drop is interpreted as seiching of the reservoir water, characterized by a period of 6.5 min with a damping ratio of 2%.

The plumb line installed at the dam indicated a relative displacement of 2.9 mm between the top of the dam and the lower inspection gallery. This relative displacement is attributable to the incremental inclination of the dam foundation induced by the near-field ground displacement.

During the strong shaking of the main shock, the vibration period of the dam body exhibited a noticeable transient increase in the upstream-downstream direction. It is probable that the change in the period resulted from changes in the hydrodynamic pressure acting on the upstream face of the dam. Further study will be required in order to examine this effect in more detail.

Acknowledgements:

The authors would like to express their thanks to the Department of Civil Engineering, Tottori Prefecture for providing valuable information regarding the effects of the 2000 earthquake on Kasho Dam. This study was partly supported by the Ministry of Education, Science, Sport and Culture of Japan through Grants-in-Aid for Scientific Research Nos. 13480119 (T. Ohmachi) and 12555134 (K. Kawashima).

References:

Geographical Survey Institute, http://www.gsi.go.jp/wnew/press-release/2000/1007-2.htm.

Inoue, D., Miyakoshi, K., Ueta, K., Miyawaki, A., and Matsuura, K. (2002), ‘‘Active fault study in the 2000 Tottori-ken seibu earthquake area, Zisin,’’ *Journal of the Seismological Society of Japan*, **5**(4), 557-573 (in Japanese).

Japan Commission on Large Dams, (2002) Acceleration records on dams and foundations No. 2 (CD-ROM version).

Lamb, H. (1932), ‘‘Hydrodynamics’’, *Cambridge Univ. Press*, 190-191.

Ohmachi, T., Kojima, N., and Murakami, A. Komaba, N. (2003), ‘‘Near-Field Effects of Hidden Seismic Faulting on a Concrete Dam,’’ *Jour. of Natural Disaster Science*, **25**(1), 7-15.

Ohmachi, T., Tsukiyama, H., and Matsumoto, H. (2001), ‘‘Simulation of tsunami induced by dynamic displacement of seabed due to seismic faulting,’’ *Bull. Seism. Soc. Am.*, **91**(6), 1898-1909.

Westergaard, H. M., (1933) ‘‘Water pressure on dams during earthquakes,’’ *Trans. ASCE* **95**, 418-433.